Clinical Biomechanics 124 (2025) 106489

Contents lists available at ScienceDirect

Clinical Biomechanics

journal homepage: www.elsevier.com/locate/clinbiomech

Distribution of strength potential of the thumb muscles and their relationship to trapeziometacarpal osteoarthritis: An exploratory cadaveric study

Mirka Normand [a,b,c,*], Mohammad Reza Effatparvar [a,b,c], Felix-Antoine Lavoie [a,b,c], Jean-Michel Brismée [d], Stéphane Sobczak [a,b,c]

[a] Département d'anatomie, Université du Québec à Trois-Rivières, Trois-Rivières, QC, Canada
[b] Chaire de recherche en anatomie fonctionnelle, Université du Québec à Trois-Rivières, Trois-Rivières, QC, Canada
[c] Groupe de recherche sur les affections neuromusculosquelettiques (GRAN), Université du Québec à Trois-Rivières, Trois-Rivières, QC, Canada
[d] Department of Rehabilitation Sciences and Center for Rehabilitation Research, School of Health Professions, Texas Tech University Health Sciences Center, Lubbock, TX, USA

ARTICLE INFO

Keywords:
Muscles
Physiological cross-sectional area
Strength distribution
Thumb
Trapeziometacarpal osteoarthritis

ABSTRACT

Background: The ten muscles of the thumb allow for a variety of movement combinations yielding similar functional outcomes yet using different load transmission with different biomechanical stresses resulting in heterogenous trapeziometacarpal wear patterns. Our exploratory study investigates the correlation between the severity and location of trapeziometacarpal joint osteoarthritis and estimated individual thumb muscles maximal force.

Method: Normalized muscle mass to body mass and physiological cross-sectional area ratio were calculated following systematic muscular dissection of 19 cadaveric hands, 60 % males, average age 79.2, SD = 7.1. Correlations were analyzed with 3 different measures of articular degenerations.

Findings: Moderate negative correlation was found between Eaton-Glickel osteoarthritis grade and normalized muscle mass of opponens pollicis ($r_s = -0.59$, $p < .01$) and abductor pollicis longus ($r_s = -0.60$, $p < .01$). Moderate negative correlation was also found between trapeziometacarpal index and normalized opponens pollicis and abductor pollicis longus muscle mass ($r_s = -0.63$, $p < .01$) and ($r_s = -0.51$, $p < .05$), respectively. No correlation was identified between physiological cross-sectional area ratios and the above degeneration metrics.

Interpretation: Our current findings identified moderate negative correlations between the normalized mass to body mass of abductor pollicis longus and opponens pollicis for both Eaton-Glickel osteoarthritis grade and trapeziometacarpal index, which would support the current hand therapy exercise recommendations for the arthritic trapeziometacarpal population. Caution must be taken in the interpretation of correlations with articular zones degradation as our analytical power was reduced by the complete eburnation of few articular surfaces.

1. Introduction

A causal relation exists between trapeziometacarpal (TMC) joint hypermobility and development of TMC joint osteoarthritis (OA) (Jonsson et al., 1996; Ladd et al., 2013; Moriatis Wolf et al., 2011; Pelligrini Jr., 1991); however laxity is not in itself abnormal and does not necessarily lead to instability (Saccomanno et al., 2013; Schmitt et al., 2008). Stability is the product of static and dynamic systems (Komatsu and Lubahn, 2018). The coordinated interaction of the ligamentous and musculotendinous systems translates in the ability to secure a joint during functional activities to allow proper control and movement (Ladd, 2018). Therefore, instability stems from issues with either or both the static and dynamic stabilizers.

An early cybernetic study, referring here to a feedback loop between the muscle and its connected sensory organ (von Foerster, 2003), on the muscular stabilization process of joints stated that the stabilizing function of muscles is often neglected in scientific works dealing with the study and modeling of human movement (Kornecki, 1992). More

* Corresponding author at: 225 Upper Pattangansett Rd, East Lyme, CT 06333, USA.
E-mail address: mirka.normand@uqtr.ca (M. Normand).

https://doi.org/10.1016/j.clinbiomech.2025.106489
Received 30 August 2024; Accepted 7 March 2025
Available online 10 March 2025

specifically, the consideration of the energy balances and the influence of individual groups of muscles on the final effect of movement (Frank et al., 2013; Kornecki, 1992). Muscular stabilization is crucial in the thumb. In fact, the thumb has multiple degrees of freedom actuated by several multiarticular muscles. While this allows several combinations yielding similar functional outcomes, it also has the potential to produce undesirable movements resulting in poor mechanics and suboptimal load transfer (Gupta and Michelsen-Jost, 2012; Kornecki, 1992; Li et al., 2008; Smutz et al., 1998a). A few thumb muscles have previously been investigated for their biomechanical effect on the TMC joint in cadavers as well as for their functional performance in vivo. Some predictable atrophies and deformities have been identified in association with TMC joint OA (Marshall et al., 2011; Mobargha et al., 2016a; Villafañe et al., 2016). Weakness of the cylindrical grasp and lateral pinch were observed in early OA, the latter of which identified as the most robust predictor of TMC OA (Ladd, 2018; McQuillan et al., 2016). Preliminary work using ultrasonographic cross-sectional measurements of the area of the thenar muscles and the first dorsal interosseous (DI-1) demonstrates atrophy of the opponens pollicis (OPP) and insertional component of the DI-1 in subjects with TMC OA (Pridgen et al., 2016). No integral profile of all thumb muscles strength has been analyzed in association with TMC OA. Refinement of our understanding of the force distribution around the thumb and its associated consequences could assist clinicians in the detection of harmful muscular imbalances and provide further objective rational to remedial recommendations, conservative or surgical.

2. Purpose of the study

The purpose of this exploratory cadaveric study was to determine if there was a correlation between the estimated individual thumb muscles maximal force ratio (through calculation of physiological cross-sectional area (PCSA) and their normalized muscle mass to body mass) with the severity and location of TMC OA. More specifically to assess the correlation between the thumb muscles PCSA ratios and normalized muscle mass with 3 different measures of articular degeneration: (1) the radiographic Eaton-Glickel OA grade, (2) the TMC index (calculation of joint degeneration based on trapezial width to height ratio), and (3) the mapping of the TMC joint articular degeneration. We hypothesized that there would be a negative correlation between the PCSA ratios and normalized muscle mass to body mass of the abductor pollicis brevis, opponens pollicis, and first dorsal interosseous with the Eaton-Glickel osteoarthritis grade and TMC index (Adams et al., 2018; Pridgen et al., 2016).

3. Methods

3.1. Selection criteria

This study was approved by the Ethics Subcommittee of the Department of Anatomy of the University of the primary investigator (SCELERA 23-07B). A sample size of 18 fresh frozen cadavers' hands had been determined a priori for an expected moderate effect size based on power calculation for a previous correlational study performed with the same subjects (Normand et al., 2023). Exclusion criteria included previous injury or surgery to the thumb or wrist.

3.2. Examiner

The dissection and fascicular measurements were performed by the principal investigator who is an experienced certified hand therapist (MN), a biomedical engineer and PhD candidate colleague (MRE), and an athletic trainer candidate (FAL), all of whom were trained in human dissection.

3.3. Procedures

Muscle architecture is recognized as the primary determinant of muscle function. PCSA was identified as being directly proportional to a muscle's maximum force in quantitative muscle architecture studies (Martin et al., 2020; Narici et al., 1992; Olson et al., 2018; Sims et al., 2018), and measurement of the PCSA has been utilized across a wide breadth of biological disciplines and was calculated using muscle volume and their pennation angle (i.e., the fiber angle relative to the force-generating axis), divided by muscle fiber length. The recommended formula per Martin et al. (2020) and Olson et al. (2018) is as follows (Martin et al., 2020; Olson et al., 2018; Payne et al., 2006):

$$\mathrm{PCSA}\left(\mathrm{cm}^2\right) = \frac{\text{muscle mass}(g) \times \text{cosine of pennation angle (rad)}}{\text{muscle density}(\mathrm{gcm}^{-3}) \times \text{fascicle lenght (cm)}}$$

Therefore, all muscles acting on the thumb were systematically dissected from superficial to deep for each specimen including, intrinsics: abductor pollicis brevis (APB), flexor pollicis brevis (FPB), opponens pollicis (OPP), adductor pollicis oblique and transverse (ADPo, ADPt), and first dorsal interosseous (DI-1), and extrinsics: abductor pollicis longus (APL), extensor pollicis brevis (EPB), extensor pollicis longus (EPL), and flexor pollicis longus (FPL). Special attention was taken to maintaining muscle moisture throughout the process with periodical misting of a phosphate-buffered saline solution to prevent desiccation during dissection.

Following the removal of each muscle and associated free tendons, total muscle mass (TMM) and specific muscle belly mass (MBM) were recorded to the nearest 0.1 g using an electronic balance (Model: AND HX-400). Fascicle length (FL) was measured at $n = 25$ random sites (Charles et al., 2022) by 3 examiners (MN, MRE, FAL) for each muscle, from digital pictures using ImageJ software (Schneider et al., 2012) (Fig. 1). As the distribution of muscle fiber length is reported not to follow a normal curve, the median value was utilized instead of the mean due to its greater statistical support (Charles et al., 2022; Kupczik et al., 2015). Lastly, all muscles pennation angles (θ: in deg) were also measured with ImageJ by a single examiner (MN) at $n = 10$ random sites between the fascicles and either the muscle long axis or internal tendon (Fig. 1) and was subsequently converted into radians for calculation. The PCSAs were tallied for all muscles and converted into ratios. Additionally, isolated muscle mass was normalized to the individual body mass for separate cross specimen comparison. Muscle mass and strength were found to be correlated in individuals over 50 years of age in the United States, regardless of the associations of age and sex (Chen et al., 2013; Riviati and Indra, 2023).

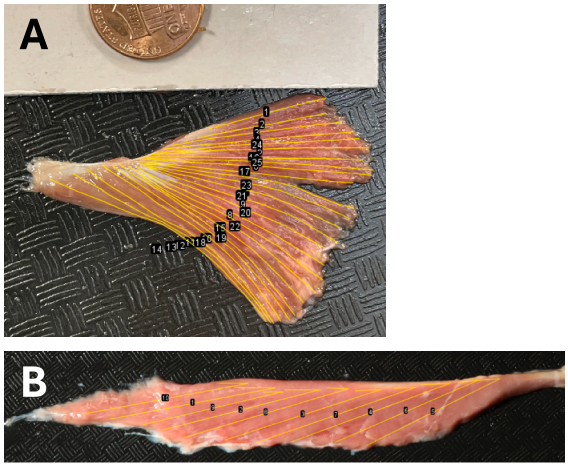

Fig. 1. Fascicle and pennation measurements with ImageJ. **A:** A penny was used for size reference for the 25 fascicle measurements. **B:** Pennation angles were measured at 10 different sites.

The following indicators of TMC joint degeneration were obtained from an earlier study by the same primary investigator using the same specimens (Normand et al., 2023). The radiographic Eaton and Glickel classification encompasses 4 stages describing the severity of TMC OA from a postero-anterior x-ray image. Stage 1: Subtle carpometacarpal joint space widening. Stage 2: Slight carpometacarpal joint space narrowing, sclerosis, and cystic changes with osteophytes or loose bodies <2 mm. Stage 3: Slight carpometacarpal joint space narrowing, sclerosis, and cystic changes with osteophytes or loose bodies >2 mm. Stage 4: Arthritic changes in the TMC joint as in Stage 3 with scaphotrapezial arthritis (Kennedy et al., 2016). And the TMC index based on trapezial width to height ratio measured from Robert's radiographic view of the TMC joint allowing clear visualization of all four trapezium articulations. A ratio of one represents a healthy joint, whereas a higher ratio indicates a more advanced disease and osteophytes development (Guang and Crisco, 2015; Ladd et al., 2015).

The articular surface integrity was also determined by direct visualization. The location of chondral lesions was described following the articular sub-division model for the TMC joint proposed by Dourthe et al. (2016) (Dourthe et al., 2016), which divides the articular surfaces

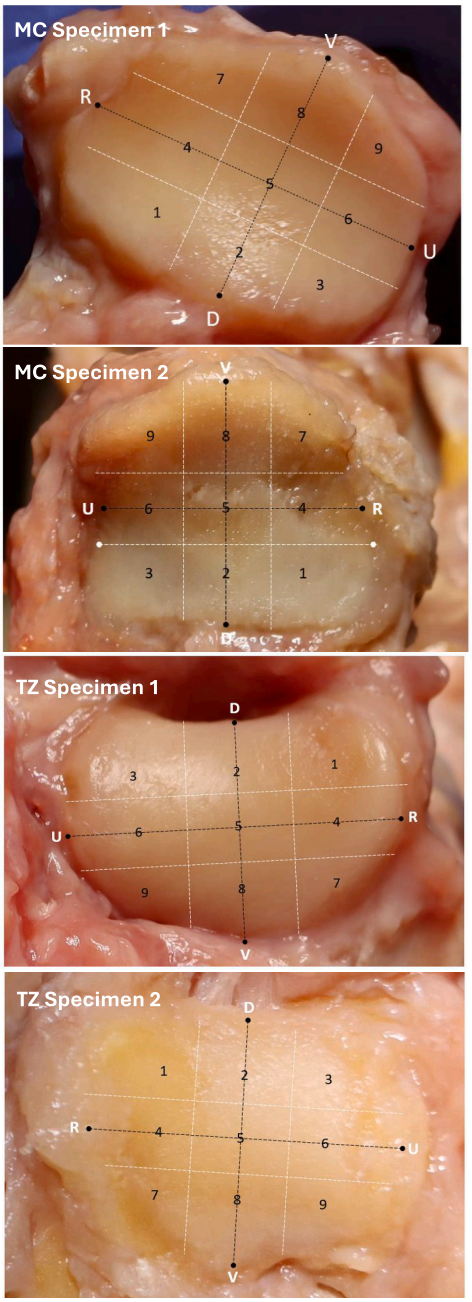

MC-1 zones	Specimen 1	Specimen 2
DR (1)	2	2
DC (2)	3	3
DU (3)	3	2
CR (4)	2	4
C (5)	2	3
CU (6)	1	4
VR (7)	3	4
VC (8)	3	4
VU (9)	2	4
TZ zones	**Specimen 1**	**Specimen 2**
DR (1)	3	4
DC (2)	2	3
DU (3)	2	4
CR (4)	3	4
C (5)	2	2
CU (6)	3	4
VR (7)	2	4
VC (8)	2	3
VU (9)	3	3

Fig. 2. First metacarpal (MC) and trapezium (TZ) articular subdivisions according to Dourthe et al. (2016), and cartilage grading according to Xu et al. (1998).
Trapezium: The dorsal-volar axis of TZ was defined based on the lowest point on the dorsal border of the subchondral surface (D) and the lowest point of the volar edge (V). The radial-ulnar axis was defined as the line perpendicular to the dorsal-volar axis which passes through its center. This axis connects the radial (R) and ulnar (U) horns of the trapezium.
First metacarpal: The dorsal-volar axis of MC was identified as the connection between the highest point on the dorsal edge of the subchondral surface (D) and the highest point of the palmar beak (V). The radial-ulnar axis was defined as the line perpendicular to the dorsal-volar axis which passes through its center. This axis connects the two lowest points of the radial (R) and ulnar (U) aspects of the MC. Dorsal radial (DR), Dorsal central (DC), Dorsal ulnar (DU), Central radial (CR), Central (C), Central ulnar (CU), Volar radial (VR), Volar central (VC), Volar ulnar (VU).

into 9 zones. The severity of the chondral lesions was graded between 1 and 4 for each zone by a single observer (MN) following the anatomic cartilage grading protocol scale presented by Xu et al. (1998) for the topographical study of osteoarthritic TMC joint. Stage 1: Normal; smooth shiny, and intact surface. Stage 2: Early cartilage degeneration; surface fibrillation, minor surface pitting. Stage 3: Progressive cartilage degeneration; deep surface pitting, fissures, clefts, surface blistering, exposed bone. Stage 4: End-stage cartilage degeneration; eburnated bone (Xu et al., 1998). (Fig. 2).

3.4. Statistical analysis

ICC estimates and their 95 % confidence intervals were calculated for the intra-rater reliability of zone grading and PCSA (ICC 3,1) based on single-rating, consistency, 2-way mixed effects model. The inter-rater reliability of PCSA (ICC 2,3) was calculated based on mean-rating, absolute agreement, 2-way mixed effects model (Koo and Li, 2016). Spearman's rho was selected for the analysis of correlations between our ordinal and continuous data, and Person correlation was used for the analysis between continuous data (Table 1). Correlation interpretation according to Chan et al (Akoglu, 2018),. poor (<0.3), fair (0.3–0.5), moderate (0.6–0.7), very strong (>0.8).

4. Results

4.1. Demographic information

19 hands from 10 cadaveric specimens were utilized for this project, 53 % right. The average specimens age was 79.2, SD = 7.1, 60 % males. The specimens exhibited different levels of TMC joint OA severity. Per the Eaton and Glickel classification, 4 specimens were rated at grade 0, 4 specimens at grade 1, 6 specimens at grade 2, 2 specimens at grade 3, and 3 specimens at grade 4. Per the TMC index, degradation ranged from 1.18 to 5.69. Degeneration presented bilaterally in all specimens although at varying adjacent degrees. Age, gender, hand dominance, smoking history, and occupational history were gathered when available (Table 2).

4.2. Correlation of PCSA ratios and normalized muscle mass to body mass with the Eaton-Glickel OA grade and the TMC index (Table 3)

No significant correlation was found between the PCSA ratios and the Eaton-Glickel OA grade nor the TMC index. However, a moderate negative correlation was found between the Eaton-Glickel OA grade and the normalized muscle mass of the opponens pollicis (OPP) ($r_s = -0.59$, $p < .01$) and the abductor pollicis longus (APL) ($r_s = -0.60$, $p < .01$). A moderate negative correlation was also found between the TMC index and the normalized OPP and APL muscle mass ($r_s = -0.63$, $p < .01$) and ($r_s = -0.51$, $p < .05$), respectively.

Table 1
Measurements reliability. Intraclass correlation coefficients (ICC) with confidence intervals.

Single Measures	Intraclass Correlation	95 % Confidence Interval	
		Lower Bound	Upper Bound
PCSA (intra-rater reliability MN)	0.99	0.97	1.0
PCSA (intra-rater reliability MRE)	1.0	1.0	1.0
PCSA (intra-rater reliability FAL)	0.99	0.95	0.99
PCSA (inter-rater reliability)	0.97	0.86	1.0
OA grading of articular zones (intra-rater reliability)	0.81	0.75	0.87

Table 2
Demographic information. (F) Female, (M) Male, (Kg) kilogram, (m) meter.

Sex	Age	Weight (Kg)	Height (m)	Dominance	Smoking	Occupation
F	87	53.6	1.55	Right	No	Teacher
M	76	75	1.72	Right	Yes	Industrial carpet and floor cleaner
M	89	77	1.72	Right	No	Electrical contractor
F	87	47.6	1.55	Unknown	Unknown	Unknown
M	74	59	1.63	Right	Unknown	Government worker
M	70	56	1.7	Right	No	Peace officer/ Farm worker
M	73	65	1.68	Right	Unknown	Agronomist
M	83	43.1	1.73	Unknown	Unknown	Truck driver
F	81	66	1.6	Right	No	Hairdresser/ Nail technician
F	72	44	1.5	Unknown	Unknown	Unknown

Table 3
Spearman's rho correlations (N = 19). Physiological cross-sectional area (PCSA), Osteoarthritis (OA), Trapeziometacarpal (TMC), Metacarpal (MC), Trapezium (TZ), Adductor pollicis transverse (ADPt), Adductor pollicis oblique (ADPo), Abductor pollicis brevis (APB), Abductor pollicis longus (APL), Opponens pollicis (OPP), Flexor pollicis longus (FPL).

Articular damage metrics	Correlation to PCSA ratio	Correlation to normalized muscle mass to body mass
Eaton-Glickel OA Grade	none	APL (−0.60**) OPP (−0.59**)
TMC Index	none	APL (−0.51*) OPP (−0.63**)
MC1: Dorso-radial	ADPt/ADPo (0.47*)	none
MC2: Dorso-central	none	none
MC3: Dorso-ulnar	none	none
MC4: Central-radial	APB (−0.47*)	none
MC5: Central	APB (−0.54*)	OPP (−0.51*)
MC6: Central-ulnar	none	APL (−0.58**)
MC7: Volar-radial	none	none
MC8: Volar-central	none	none
MC9: Volar-ulnar	none	APL (−0.48*)
TZ1: Dorso-radial	none	OPP (−0.58*)
TZ2: Dorso-central	none	none
TZ3: Dorso-ulnar	none	OPP (−0.56*)
TZ4: Central-radial	none	OPP (−0.68**)
TZ5: Central	none	none
TZ6: Central-ulnar	none	FPL (−0.46*), APL (−0.53*)
TZ7: Volar-radial	none	OPP (−0.60**)
TZ8: Volar-central	APB (−0.47*)	none
TZ9: Volar-ulnar	none	none

** . Correlation is significant at the 0.01 level (2-tailed).
* . Correlation is significant at the 0.05 level (2-tailed).

4.3. Correlation of PCSA ratios and normalized muscle mass to body mass with the location and severity of TMC articular degeneration (Table 3)

A moderate negative correlation was found between the PCSA of APB and the articular damage of the central zone of the first metacarpal (MC) ($r_s = -0.54$, $p < .05$). A fair negative correlation was found between the combined PCSA of ADPt/ADPo and the dorso-radial zone of the first MC ($r_s = -0.47$, $p < .05$). A fair negative correlation was also found between the PCSA of APB and the central-radial MC and the volar-central trapezial zones, both ($r_s = -0.47$, $p < .05$).

A moderate negative correlation was observed between the normalized muscle mass of APL and OPP with the following zones: APL-MC central-ulnar ($r_s = -0.58$, $p < .01$), and TZ central-ulnar ($r_s = -0.53$, $p < .05$). OPP- MC central ($r_s = -0.51$, $p < .05$), TZ dorso-radial

($r_s = -0.58$, $p < .05$), TZ dorso-ulnar ($r_s = -0.56$, $p < .05$). TZ central-radial ($r_s = -0.68$, $p < .01$), and TZ volar-radial ($r_s = -0.60$, $p < .01$).

5. Discussion

5.1. Correlation of PCSA ratios and normalized muscle mass to body mass with the Eaton-Glickel OA grade and the TMC index

Although we found moderate to strong correlation between the PCSA ratios and normalized muscle mass to body mass ratios for most muscles, different correlations were found between the articular damage metrics and our two maximum muscular force estimation methods. TMC OA is often thought of as a disease of aging that is mechanical in origin (Felson and Felson, 2013), however, it is possible that some of the mechanical changes that appear over time were the result of normal aging including sarcopenia and other TMC OA risks factors (Wilson et al., 2013). Additionally, it should be considered that muscular atrophy could be the result of long standing pain and joint deformity accompanying TMC OA disease process, and not necessarily a causality. Therefore, we support continued exploration of this relationship in future research.

5.2. Correlation of PCSA ratios and their normalized muscle mass to body mass with the location of degeneration of the TMC articular surfaces

Several TMC joints ($n = 6$) presented complete eburnation of both articular surfaces, which reduced our sample size by 30 % for the articular cartilage wear mapping analysis. We therefore recommend considering those results with more reservation.

The cartilage areas of negative correlation with APB corresponds with the location of engagment of the volar beak with the trapezium at end range of opposition, and was identified in previous reasearch as having the highest shear contact (Edmunds, 2011; Pelligrini Jr., 1991; Xu et al., 1998). Our findings suggest that APB may assist in better dispersal of force on the cartilage surface (Wilson et al., 2013), through its palmar abduction motion bringing the first metacarpal in a more optimal alignment to the orientation of the trapezial articular surface, facing a palmar and radial direction (Duerinckx and Caekebeke, 2016).

Regarding correlations with the normalized muscle mass to body mass, OPP presented moderate negative correlation with several MC and TZ zones. OPP is one of the agonist of the first phase of the screw home torque mechanism, which consists of pronation of the first metacarpal causing axial compression and increased joint congruence via tightening of the stabilizing ligaments (Edmunds, 2011). Our findings align with results from sonographic assessments of the thenar muscles of subjects with TMC OA (Lai et al., 2022; Pridgen et al., 2016), and by extrapolation would support the growing body of evidence in favor of isolated strengthening of that muscle in hand therapy (Adams et al., 2018; Mobargha et al., 2016b). Although we find evidence in favor of OPP strengthening (Adams et al., 2018; McGee et al., 2015; Mobargha et al., 2016a), it is also reported that the pronation ability of the first metacarpal diminishes with increasing joint degeneration (Normand et al., 2023). Therefore, the benefits of its strengthening may vary. As for the APL muscle mass, its moderate negative correlation with degradation of the ulnar border of the MC cartilage as well as the central-ulnar TZ zone, could also be explained by its palmar abduction influence, offloading the ulnar border of the joint as it orients the MC more congruently to the trapezium.

5.3. Correlations between all PCSA ratios

When examining the correlations between all PCSA ratios (Table 4), we discovered an antagonistic relationship between ADPo and EPB. Diametrically opposed within the flexion/adduction and extension/radial abduction plane of motion of the first MC (Neumann and Bielefeld, 2003; Smutz et al., 1998b), their directional affinity align with mechanical patterns of flexion or hyperextension of the metacarpophalangeal joint observed clinically. We speculate that patterns of dominance of either intrinsic or extrinsic action during grip and pinch create different load transmission and biomechanical stresses leading to different wear patterns. As such, a dominant adductor would most likely be associated with hyperextension of the metacarpophalangeal (MCP) joint (Moulton et al., 2001; Pellegrini Jr. et al., 1996). Conversely, a dominant extrinsic would orient the metacarpal in a more radially abducted position encouraging flexion of the MCP joint during function, which has been reported to transfer the load more dorsally and decrease shear forces (Kerkhof et al., 2022; Moulton et al., 2001).

Table 4
Correlations between physiological cross section area (PCSA) ratios with their respective confidence intervals ($N = 19$). Extensor pollicis brevis (EPB), Adductor pollicis transverse (ADPt), Adductor pollicis oblique (ADPo), First dorsal interosseous (DI-1).

Correlations with confidence intervals				
PCSA Ratios	Pearson correlation	Sig. (2-tailed)	95 % Confidence Intervals (2-tailed)	
			Lower	Upper
EPB and ADPt	0.52	0.02	0.08	0.79
EPB and ADPo	−0.59	0.01	−0.82	−0.18
EPB and DI-1	0.46	0.05	0.01	0.76
ADPt and ADPo	−0.62	0.00	−0.84	−0.24

5.4. Limitations

Data obtained from elderly individuals reduces our ability to generalize our results to the wider population. Additionally, several TMC joints ($n = 6$) presented complete eburnation of both articular surfaces, reducing our sample size by 30 % for the articular cartilage degeneration mapping analysis.

The manual dissection of fresh specimen is delicate and exposes them to potential damage and dehydration. We sougth to minimize the dehydration with periodical moistening.

The method selected for the PCSA calculation utilized a limited sample of muscle fibers ($N = 25$) compared to higher fiber numbers ($n > 1000$) obtained from those using medical imaging data. Our PCSA calculation method could have introduced errors by not accurately characterizing the architecture of the muscles. However, despite a seemingly small number of muscle fibers, this measurement technique provided thorough coverage of our digital muscle images through ImageJ.

The measurement of the muscle pennation angles, which was performed outside of its physiological environment could have led to some over or under estimation of the angulation, affecting the results of the PCSA calculation. However, this potential source of error was minimized by having each researcher take pictures of the muscles immediately after their removal, in the position that was observed during dissection.

6. Conclusions

Our current findings identified moderate negative correlations between the normalized mass to body mass of APL and OPP for both Eaton-Glickel OA grade and TMC index, which supports the current hand therapy recommendations pertaining to stabilization of the TMC joint for OA population (Neumann and Bielefeld, 2003; O'Brien et al., 2022; O'Brien and Giveans, 2013; Valdes and von der Heyde, 2012). Regarding correlations with the articular zone damage of MC and TZ, caution in the results interpretation is recommended. Although the APB PCSA ratio and APL and OPP normalized muscle mass to body mass were identified as having fair to moderate negative correlation with several zones' degeneration of the MC and TZ articular surfaces, the reduced size of our sample caused by the complete articular eburnation of 6 of

our 19 specimens negatively affect the generalizability of those observations. The discovery of a reverse relationship of PCSA ratio between the ADPo and the EPB was interesting as it is reminiscent of directionally opposite movement strategies observed in vivo. Finally, we are reminded that our analysis of the individual thumb muscles could not account for the results of their combined action. We would be remiss to overlook the impact of its infinite number of kinematic combinations, which most certainly affects the load distribution and rate of degeneration. Future research should consider larger samples and more inclusive assessment of the thumb's directional force distribution in vivo and its associated movement patterns to help us better understand which combinations drive deformity and provide further scientific data to support its remediation.

CRediT authorship contribution statement

Mirka Normand: Writing – review & editing, Writing – original draft, Methodology, Investigation, Formal analysis, Data curation, Conceptualization. **Mohammad Reza Effatparvar:** Investigation, Formal analysis, Data curation. **Felix-Antoine Lavoie:** Investigation, Formal analysis, Data curation. **Jean-Michel Brismée:** Writing – review & editing, Validation, Supervision, Methodology, Conceptualization. **Stéphane Sobczak:** Writing – review & editing, Validation, Supervision, Methodology, Formal analysis, Conceptualization.

Declaration of competing interest

The authors declare that they have no known competing financial interests or personal relationships that could have appeared to influence the work reported in this paper.

Appendix A. Supplementary data

Supplementary data to this article can be found online at https://doi.org/10.1016/j.clinbiomech.2025.106489.

References

Adams, J.E., O'Brien, V., Magnusson, E., et al., 2018. Radiographic analysis of simulated first dorsal interosseous and Opponens Pollicis loading upon thumb CMC joint subluxation: a cadaver study. Hand (New York, NY) 13, 40–44. https://doi.org/10.1177/1558944717691132.

Akoglu, H., 2018. User's guide to correlation coefficients. Turk. J. Emerg. Med. 18, 91–93. https://doi.org/10.1016/j.tjem.2018.08.001.

Charles, J., Kissane, R., Hoehfurtner, T., et al., 2022. From fibre to function: are we accurately representing muscle architecture and performance? Biol. Rev. 97, 1640–1676. https://doi.org/10.1111/brv.12856.

Chen, L., Nelson, D.R., Zhao, Y., et al., 2013. Relationship between muscle mass and muscle strength, and the impact of comorbidities: a population-based, cross-sectional study of older adults in the United States. BMC Geriatr. 13, 74. https://doi.org/10.1186/1471-2318-13-74.

Dourthe, B., D'Agostinoa, P., Stockmansa, F., et al., 2016. In vivo contact biomechanics in the trapeziometacarpal joint using finite deformation biphasic theory and mathematical modelling. Med. Eng. Phys. 38, 108–114. https://doi.org/10.1016/j.medengphy.2015.11.003.

Duerinckx, J., Caekebeke, P., 2016. Trapezium anatomy as a radiographic reference for optimal cup orientation in total trapeziometacarpal joint arthroplasty. J. Hand Surg. Eur. 41, 939–943. https://doi.org/10.1177/1753193416630496.

Edmunds, J.O., 2011. Current concepts ofthe anatomy ofthe thumb trapeziometacarpal joint. J. Hand. Surg. [Am.] 36, 170–182. https://doi.org/10.1016/j.jhsa.2010.10.029.

Felson, D.T., Felson, D.T., 2013. Osteoarthritis as a disease of mechanics. Osteoarthr. Cartil. 21, 10–15. https://doi.org/10.1016/j.joca.2012.09.012.

Frank, C., Kobesova, A., Kolar, P., 2013. Dynamic neuromuscular stabilization & sports rehabilitation. Int. J. Sports Phys. Ther. 8, 62–73.

Guang, S., Crisco, T., 2015. Radiographic evaluation of the carpometacarpal joint in early stage osteoarthritis severity and joint laxity. R I Med. J. 98, 23–24 (2015/08/01).

Gupta, S., Michelsen-Jost, H., 2012. Anatomy and function of the Thenar muscles. Hand Clin. 28, 1–7. https://doi.org/10.1016/j.hcl.2011.09.006.

Jonsson, H., Valtysdottir, S.T., Kjartansson, O., et al., 1996. Hypermobility associated with osteoarthritis of the thumb base: a clinical and radiological subset of hand osteoarthritis. Ann. Rheum. Dis. 55, 540–543.

Kennedy, C.D., Manske, M.C., Huang, J.I., 2016. Classifications in brief: the eaton-littler classification of thumb carpometacarpal joint arthrosis. Clin. Orthop. Relat. Res. 474, 2729–2733. https://doi.org/10.1007/s11999-016-4864-6.

Kerkhof, F., Kenney, D., Ogle, M., et al., 2022. The biomechanics of osteoarthritis in the hand: implications and prospects for hand therapy. J. Hand Ther. 35, 367–376. https://doi.org/10.1016/j.jht.2022.11.007.

Komatsu, I., Lubahn, J.D., 2018. Anatomy and biomechanics of the thumb carpometacarpal joint. Oper. Tech. Orthop. 28, 1–5. https://doi.org/10.1053/j.oto.2017.12.002.

Koo, T.K., Li, M.Y., 2016. A guideline of selecting and reporting intraclass correlation coefficients for reliability research. J. Chiropr. Med. 15, 155–163. https://doi.org/10.1016/j.jcm.2016.02.012.

Kornecki, S., 1992. Mechanism of muscular stabilization process in joints. J. Biomech. 25, 235–245.

Kupczik, K., Stark, H., Mundry, R., et al., 2015. Reconstruction of muscle fascicle architecture from iodine-enhanced microCT images: a combined texture mapping and streamline approach. J. Theor. Biol. 382, 34–43. https://doi.org/10.1016/j.jtbi.2015.06.034.

Ladd, A.L., 2018. The teleology of the thumb: on purpose and design. J. Hand. Surg. [Am.] 43, 248–259. https://doi.org/10.1016/j.jhsa.2018.01.002.

Ladd, A.L., Weiss, A.-P.C., Crisco, J.J., et al., 2013. The thumb carpometacarpal joint: anatomy, hormones, and biomechanics. AAOS Instr. Course Lect. 165–179.

Ladd, A.L., Messana, J., Berger, A.J., et al., 2015. Correlation of clinical disease severity to radiographic thumb osteoarthritis index. J. Hand. Surg. [Am.] 40, 474–482. https://doi.org/10.1016/j.jhsa.2014.11.021.

Lai, C., Kenney, D., Kerkhof, F., et al., 2022. Ultrasound of thumb muscles and grasp strength in early thumb carpometacarpal osteoarthritis. J. Hand Surg. 47 (898), e891–898.e898. https://doi.org/10.1016/j.jhsa.2021.07.021.

Li, Z.-M., Tang, J., Chakan, M., et al., 2008. Complex, multidimensional thumb movements generated by individual extrinsic muscles. J. Orthop. Res. 26, 1289–1295. https://doi.org/10.1002/jor.20641.

Marshall, M., van der Windt, D., Nicholls, E., et al., 2011. Radiographic thumb osteoarthritis: frequency, patterns and associations with pain and clinical assessment findings in a community-dwelling population. Rheumatology 50, 735–739. https://doi.org/10.1093/rheumatology/keq371.

Martin, M.L., Travouillon, K.J., Fleming, P.A., et al., 2020. Review of the methods used for calculating physiological cross-sectional area (PCSA) for ecological questions. J. Morphol. 281, 778–789. https://doi.org/10.1002/jmor.21139.

McGee, C., O'Brien, V., Van Nortwick, S., et al., 2015. First dorsal interosseous muscle contraction results in radiographic reduction of healthy thumb carpometacarpal joint. J. Hand Ther. 28, 375–381. https://doi.org/10.1016/j.jht.2015.06.002.

McQuillan, T., Kenney, D., Crisco, J., et al., 2016. Weaker functional pinch strength is associated with early thumb carpometacarpal osteoarthritis. Clin. Orthop. Relat. Res. 474, 557–561. https://doi.org/10.1007/s11999-015-4599-9.

Mobargha, N., Esplugas, M., Garcia-Elias, M., et al., 2016a. The effect of individual isometric muscle loading on the alignment of the base of the thumb metacarpal: a cadaveric study. J. Hand Surg. Eur. 41E, 374–379. https://doi.org/10.1177/1753193415597114.

Mobargha, N., Esplugas, M., Garcia-Elias, M., et al., 2016b. The effect of individual isometric muscle loading on the alignment of the base of the thumb metacarpal: a cadaveric study. J. Hand Surg. Eur. 41, 374–379. https://doi.org/10.1177/1753193415597114.

Moriatis Wolf, J., Schreier, S., Tomsick, S., et al., 2011. Radiographic laxity ofthe Trapeziometacarpal joint is correlated with generalized joint hypermobility. J. Hand Surg. 36A, 1165–1169. https://doi.org/10.1016/j.jhsa.2011.03.017.

Moulton, M.J.R., Parentis, M.A., Kelly, M.J., et al., 2001. Influence of metacarpophalangeal joint position on basal joint-loading in the thumb. J. Bone Joint Surg. 83-A, 709–716.

Narici, M.V., Landoni, L., Minetti, A.E., 1992. Assessment of human knee extensor muscles stress from in vivo physiological cross-sectional area and strength measurements. Eur. J. Appl. Physiol. Occup. Physiol. 65, 438–444. https://doi.org/10.1007/BF00243511.

Neumann, D.A., Bielefeld, T., 2003. The carpometacarpal joint of the thumb: stability, deformity, and therapeutic intervention. J. Orthop. Sports Phys. Ther. 33, 386–399. https://doi.org/10.2519/jospt.2003.33.7.386.

Normand, M., Ibrahim, M., Morsy, M., et al., 2023. The trapeziometacarpal screw home torque mechanism as a clinical indicator of the posterior joint ligament complex integrity: a cadaveric investigation. J. Hand Ther. https://doi.org/10.1016/j.jht.2023.08.007.

O'Brien, V.H., Giveans, M.R., 2013. Effects of a dynamic stability approach in conservative intervention of the carpometacarpal joint of the thumb: a retrospective study. J. Hand Ther. 26, 44–52. https://doi.org/10.1016/j.jht.2012.10.005.

O'Brien, V., Johnson, J., Pisano, K., et al., 2022. Dynamic stabilization of the painful thumb: a historical and evidence-informed synthesis. J. Hand Ther. https://doi.org/10.1016/j.jht.2022.06.007.

Olson, R.A., Glenn, Z.D., Cliffe, R.N., et al., 2018. Architectural properties of sloth forelimb muscles (Pilosa: Bradypodidae). J. Mamm. Evol. 25, 573–588. https://doi.org/10.1007/s10914-017-9411-z.

Payne, R.C., Crompton, R.H., Isler, K., et al., 2006. Morphological analysis of the hindlimb in apes and humans. I. Muscle architecture. J. Anat. 208, 709–724. https://doi.org/10.1111/j.1469-7580.2006.00563.x.

Pellegrini Jr., V.D., Parentis, M., Judkins, A., et al., 1996. Extension metacarpal osteotomy in the treatment of trapeziometacarpal osteoarthritis: a biomechanical study. J. Hand Surg. 21, 16–23. https://doi.org/10.1016/S0363-5023(96)80149-3.

Pelligrini Jr., V.D., 1991. Osteoarthritis of the trapeziometacarpal joint: the pathophysiology of articular cartilage degeneration. II. Articular wear patterns in the

osteoarthritic joint. J. Hand. Surg. [Am.] 16, 975–982. https://doi.org/10.1016/s0363-5023(10)80055-3.
Pridgen, E., Kenney, D., Roh, E., et al., 2016. In vivo measurement of the thenar muscles and first dorsal interosseous in thumb carpometacarpal joint osteoarthritis using ultrasound imaging. In: AAHS Annual Meeting Scottsdale, Arizona.
Riviati, N., Indra, B., 2023. Relationship between muscle mass and muscle strength with physical performance in older adults: a systematic review. SAGE Open Med. 11, 20503121231214650. https://doi.org/10.1177/20503121231214650.
Saccomanno, M.F., Fodale, M., Capasso, L., et al., 2013. Generalized joint laxity and multidirectional instability of the shoulder. Joints 1, 171–179. https://doi.org/10.11138/jts/2013.1.4.171.
Schmitt, L.C., Fitzgerald, G.K., Reisman, A.S., et al., 2008. Instability, laxity, and physical function in patients with medial knee osteoarthritis. Phys. Ther. 88, 1506–1516. https://doi.org/10.2522/ptj.20060223.
Schneider, C.A., Rasband, W.S., Eliceiri, K.W., 2012. NIH Image to ImageJ: 25 years of image analysis. Nat. Methods 9, 671–675. https://doi.org/10.1038/nmeth.2089.
Sims, D.T., Onambélé-Pearson, G.L., Burden, A., et al., 2018. Specific force of the vastus lateralis in adults with achondroplasia. J. Appl. Physiol. 124, 696–703. https://doi.org/10.1152/japplphysiol.00638.2017.
Smutz, W.P., Kongsayreepong, A., Hughes, R.E., et al., 1998a. Mechanical advantage of the thumb muscles. J. Biomech. 31, 565–570.
Smutz, W.P., Kongsayreepong, A., Hughes, R.E., et al., 1998b. Mechanical advantage of the thumb muscles. J. Biomech. 31, 565–570. https://doi.org/10.1016/s0021-9290(98)00043-8.
Valdes, K., von der Heyde, R., 2012. An exercise program for carpometacarpal osteoarthritis based on biomechanical principles. J. Hand Ther. 25, 251–263. https://doi.org/10.1016/j.jht.2012.03.008.
Villafañe, J.H., Cantero-Tellez, R., Negrini, S., et al., 2016. From art to science: the functional damage due to thumb osteoarthritis finely described by Velazquez 300 years before its clinical description. Reumatismo 69, 137–139.
von Foerster, H., 2003. Ethics and second-order cybernetics. In: von Foerster, H. (Ed.), Understanding Understanding: Essays on Cybernetics and Cognition, New York, NY. Springer New York, pp. 287–304.
Wilson, D.R., McWalter, E.J., Johnston, J.D., 2013. The measurement of joint mechanics and their role in osteoarthritis genesis and progression. Rheum. Dis. Clin. N. Am. 39, 21–44. https://doi.org/10.1016/j.rdc.2012.11.002.
Xu, L., Strauch, R.J., Ateshian, G.A., et al., 1998. Topography of the osteoarthritic thumb carpometacarpal joint and its variations with regard to gender, age, site, and osteoarthritic stage. J. Hand Surg. 23, 454–464. https://doi.org/10.1016/S0363-5023(05)80463-0.